Title

Chemically activatable viral capsid functionalized for cancer targeting

Journal

Nanomedicine, 11(4)

ISSN

1743-5889

Authors

Chen, Chun-Chieh

Xing, Li

Stark, Marie

et al.

Publication Date

2016-02-01

DOI

10.2217/nnm.15.207

Peer reviewed

Research Article

For reprint orders, please contact: reprints@futuremedicine.com

Nanomedicine

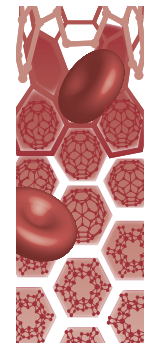

Chemically activatable viral capsid functionalized for cancer targeting

Aim: To design a theranostic capsule using the virus-like nanoparticle of the hepatitis E virus modified to display breast cancer cell targeting functional group (LXY30). **Methods:** Five surface-exposed residues were mutated to cysteine to allow conjugation to maleimide-linked chemical groups via thiol-selective linkages. Engineered virus-like nanoparticles were then covalently conjugated to a breast cancer recognized ligand, LXY30 and an amine-coupled near-infrared fluorescence dye. **Results:** LXY30-HEV VLP was checked for its binding and entry to a breast cancer cell line and for tumor targeting *in vivo* to breast cancer tissue in mice. The engineered virus-like nanoparticle not only targeted cancer cells, but also appeared immune silent to native hepatitis E virus antibodies due to epitope disruption at the antibody-binding site. **Conclusion:** These results demonstrate the production of a theranostic capsule suitable for cancer diagnostics and therapeutics based on surface modification of a highly stable virus-like nanoparticle.

Chun-Chieh Chen[1], Li Xing[1], Marie Stark[1], Tingwei Ou[1], Prasida Holla[1], Kai Xiao[2], Shizuo G Kamita[3], Bruce D Hammock[3], Kit Lam[2] & R Holland Cheng*[,1]

[1]Department of Molecular & Cellular Biology, University of California, 1 Shields Ave, Davis, CA 95616, USA

[2]Department of Internal Medicine, University of California Davis, Sacramento, CA 95817, USA

[3]Department of Entomology & Nematology, University of California, 1 Shields Ave, Davis, CA 95616, USA

*Author for correspondence: rhch@ucdavis.edu

First draft submitted: 2 July 2014; **Accepted for publication:** 14 December 2015; **Published online:** 20 January 2016

Keywords: cycloaddition of targeting ligand • cysteine replacement • hepatitis E • multivalent ligand display • virus-like particle

Background

Cancer theranostics require specific targeting of drug/diagnostic element to tumor cells specifically, without binding to or affecting healthy cells and tissues. Most delivery systems provide feasible, yet low specificity, solutions. They are usually based on liposome and/or organic polymers such as polyethylene glycol. Virus-like particles (VLPs) have been used as nanocarriers to display foreign epitopes and/or deliver small molecules in a highly specific manner for use as vaccines or therapeutic agents against disease phenotypes [1]. This is facilitated mainly by their ability to self-assemble and the ease of genetically modifying them. Hepatitis E virus (HEV) is composed of a nonenveloped icosahedral capsid, enclosing a single-stranded RNA genome of 7.2 kilobases [2]. The major capsid protein is encoded by the second open reading frame (ORF2) and is essential not only for virus assembly, but also for immunogenicity and host interaction [3]. The recombinant capsid protein (CP) is able to self-assemble into virus-like particles when expressed in insect cells after deletion of 111 amino acids from the N-terminal end and 52 amino acids from the C-terminal end. CP folds into three domains: S (shell; amino acids 118-317), M (middle; amino acids 318-451) and P (protruding; amino acids 452-606 [4–6].

The S-domain forms a typical antiparallel beta-barrel structure and assembles into stable icosahedral shell, while the P-domain protrudes as a surface spike that profoundly determines HEV antigenicity. The M-domain appears as plateau residing at the threefold of the icosahedral capsid and the function is not known yet. With three-

Future Medicine part of fsg

domain modularity, HEV-VLP can easily maneuver its assembly with antigenicity, in other words, size reduction from T = 3 to T = 1 icosahedral particle without changing in antigenicity [7]. Administration of HEV-VLP in nonhuman primates elicits both systemic and mucosal immunity with undetectable tolerance, as well as protection against HEV challenge [8]. Moreover, it can accommodate sequence modification at P-domain without interference with HEV-VLP assembly. Genetically engineered chimeric VLPs having modifications in the somewhat isolated protrusion domain, are as stable as wild-type VLPs [9], and like the HEV virion, can tolerate extreme pH values and intestinal proteases [10]. This has exciting implications for an orally deliverable chemotherapeutic agent. All this evidence makes it feasible to use the HEV-VLP as a scaffold for modification of its protrusion domain as exterior contact points for cancer targeting (for diagnostics or therapeutics). The functionalized VLP can encapsulate drugs, DNA/RNA or inorganic beads as targeted cargo delivery system.

In this study, we created a theranostic capsule whose targeting specificity was altered by chemically conjugating the targeting ligand onto its exterior surface. Specifically, HEV-VLP was engineered to have an exposed cysteine residue in one of the surface variable loops of the P-domain. Of the five mutants generated, the N573C was found to be most suited for conjugation of chemical groups by a thiol-selective reaction and subsequent secondary binding of ligands to the conjugated groups. The LXY30 ligand peptide was conjugated to the N573C-VLP, allowing enhanced affinity to human malignant breast tumor cells [11] as well as *in vivo* to tumor tissue, indicating that delivery route of virus-like particle can be manipulated to facilitate targeted delivery to pathologic foci.

Methods

Site-directed mutagenesis of the P domain of dORF2-HEV

Five amino acid residues (Y485, T489, S533, N573 and T586) of the P-domain were individually mutated to a cysteine residue by site-directed mutagenesis using a QuikChange site-directed mutagenesis kit (Stratagene) following the manufacturer's protocols. The baculovirus transfer vector carrying the *dORF2* gene (pFastBac1/dORF2-HEV) was used as template for the site-directed mutagenesis [12]. These residues were chosen for mutagenesis on the basis of the dimer model and crucial binding site information of HEV [13]. The forward and reverse primers for each site-directed mutagenesis reaction are shown in Supplementary Table 1. The mutated pFastBac1/dORF2-HEV plasmids carrying the site mutations Y485, T489, S533, N573 and T586 were named pFastBac1/dORF2-HEV-Y485, -T489, -S533, -N573 and -T586, respectively. The authenticity of each mutation in these plasmids was confirmed by sequencing of both strands.

Production & purification of HEV-Cys-VLPs & *in vitro* disassembly

The mutated CP was expressed in insect High Five cells (Invitrogen™, CA, USA) using baculovirus-based expression vectors. The recombinant baculoviruses used to express the mutated CPs were generated using the Bac-to-Bac® Baculovirus Expression System on *Sf*9 cells (Invitrogen) and each of the pFastBac1/dORF2-HEV plasmids described above according to the protocols supplied by the manufacturer. The *Sf*9 and High Five cells were maintained on ESF921 medium (Expression Systems, CA USA) and Excell 420 medium (SAFC Biosciences, KS, USA) supplemented with 2.5% heat-inactivated fetal bovine serum (FBS), respectively, following standard protocols [14]. The production and purification of HEV-Cys-VLPs from the various mutated POR2 constructs were conducted as described previously [15]. In order to express the mutated POR2 proteins and generate VLPs, the High Five cells were inoculated with each baculovirus construct at a multiplicity of infection of 5 and cultured for 6–7 days. The VLPs were collected and purified through multiple steps of CsCl equilibrium density-gradient ultracentrifugation as described previously [16]. The purified VLPs were resuspended in 10 mM potassium-MES buffer, pH = 6.2 and stored at 4°C. The purified VLPs were disrupted by dialysis against buffer containing EDTA (10 mM) or/and DTT (20 mM). A mini dialysis device (Millipore) was used in the disassembly experiments.

Chemical conjugation of maleimide-linked biotin onto HEV-Cys VLPs via thiol reaction

Maleimide-linked biotin (20–200 µM) was used to react with HEV-Cys VLPs (4–40 µM) in 0.01 M PBS, pH = 7.2 at 4°C overnight. Unbound maleimide-biotin was then removed using a 7000 MWCO desalting column (Zeba™ Spin Desalting Columns, Thermo Scientific, MA, USA).

Preparation of LXY30-VLP–Cy5.5 complexes for flow cytometric analysis, cell tests & *in vivo* imaging on mice

Six hundred fifty micrometers maleimide-azide and 650 µM alkyne-LXY30 in the presence of 200 µM $CuSO_4$ and 1 mM ascorbic acid were incubated at 4°C overnight. Then maleimide-conjugated LXY30 was added at molar ratio of 3:1 (ligand vs binding site) to react with the Cys residues on HEV-Cys mutants though a thiol

reaction at 4°C overnight. The unconjugated molecules were removed by a 7000 MWCO desalting column (Zeba Spin Desalting Columns, Thermo Scientific).

To chemically conjugate Cy5.5 NHS ester (Limiprobe) to HEV-Cys VLPs, Cy5.5 NHS ester (200 nM) was used to react with HEV-Cys mutants (20 µM) at molar ratio of 300:1 (dye vs VLP) in buffer containing 0.01 M PBS, pH = 7.2 at room temperature for 2 h, followed by incubation at 4°C overnight. The free Cy5.5 NHS ester was then removed by a 7000 MWCO desalting column (Zeba Spin Desalting Columns, Thermo Scientific).

Flow cytometric analysis

MDA-MB-231 breast cancer cells were incubated with Cy5.5-labeled HEV-573C-VLPs (VLP-Cy5.5) or Cy5.5/LXY30-conjugated HEV-573C-VLPs (LXY3-VLP-Cy5.5) for 1 h at 37°C, respectively. Then the cells were washed with PBS three times and resuspended in PBS for the flow cytometric analysis [11]. A total of 10,000 events were collected for each sample. Unstained cells were used as a control.

Confocal microscopy

The sample preparation was performed according to previously established protocol [16]. Briefly, MDA-MB-231 breast cancer cells were seeded in the coverglass chamber slides (VWR LabShop, IL, USA). After reaching 80% confluence, the cells were incubated with Cy5.5-labeled HEV-573C-VLPs (VLP-Cy5.5) and Cy5.5-labeled LXY30-conjugated HEV-573C-VLPs (LXY3-VLP-Cy5.5), respectively for 1 h at 37°C. The cell nuclei were stained with Hoechst 33342 (Invitrogen) for 5 min. The cells were washed twice with PBS and replaced with fresh medium before observation under a Zeiss confocal fluorescence microscope.

In vivo optical imaging

Female SPF BALB/c mice, 6–8 weeks of age, were purchased from Charles River (CA, USA) and kept

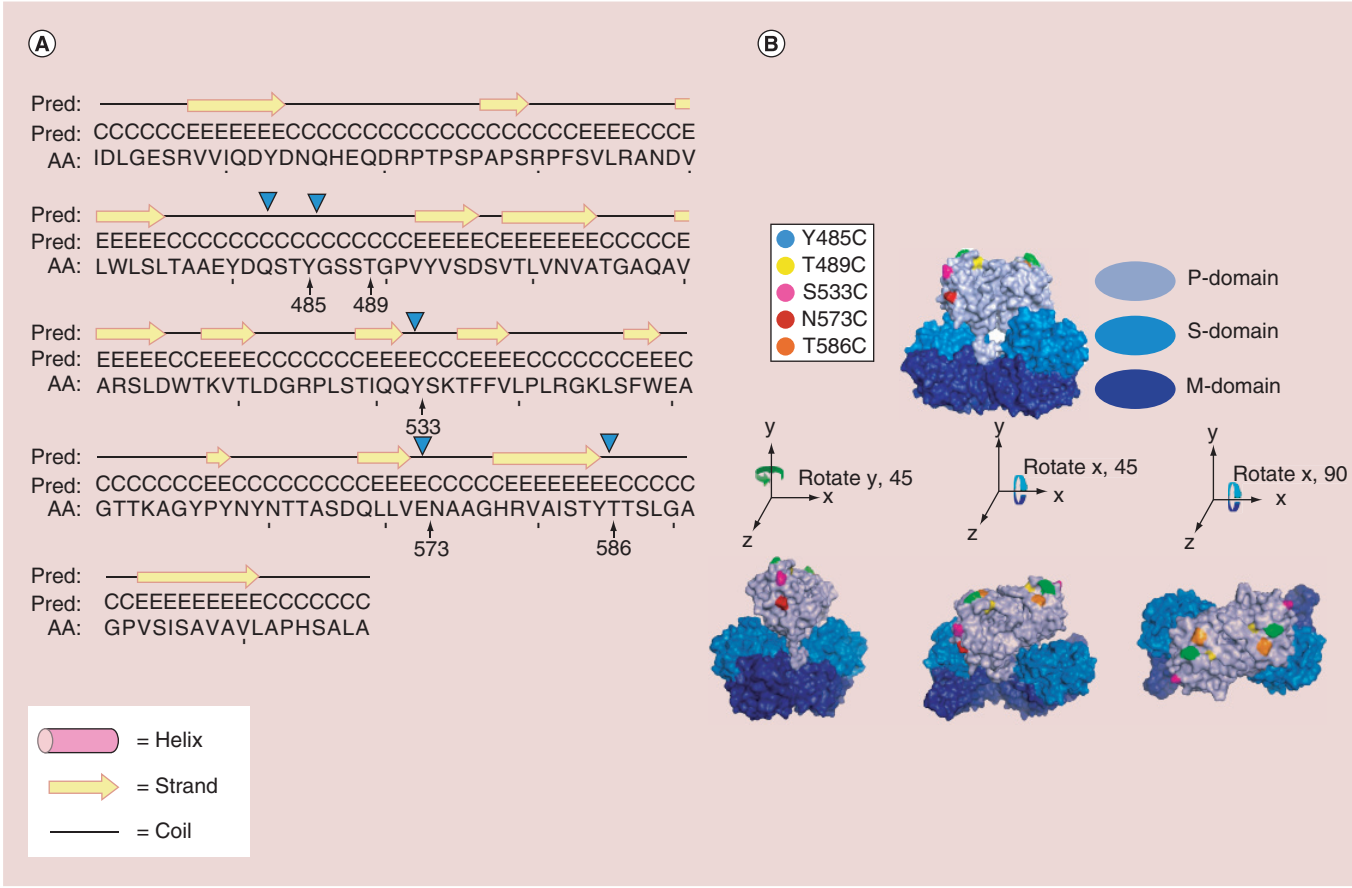

Figure 1. Cysteine replacement on surface protrusion domain of hepatitis E virus virus-like particle. Cysteine mutation was proposed on residues Y485, T489, S533, N573 and T586 at flexible coil region to minimize the disturbance to the secondary structure of capsid protein **(A)**. The residue N573 is located in proximity to the binding site of HEP230. All the selected residues for cysteine mutation were located at the surface of the P-domain, with residue Y485 (cyan), T489 (yellow), T586 (orange) on the outmost surface, and residues S533 (magenta) and N573 (red) at side facing virus-like particle fivefold axis **(B)**.
AA: Target sequence; Pred: Predicted secondary structure.

under pathogen-free conditions according to Association for Assessment and Accreditation of Laboratory Animal Care (AAALAC) guidelines and were allowed to acclimatize for at least 4 days prior to any experiments. MDA-MB-231 breast cancer cells (5×10^5) were injected into the mammary fat pad of female nude mice. All animal experiments were performed in compliance with institutional guidelines and according to protocol no. 17222 approved by the Animal Use and Care Administrative Advisory Committee at the University of California, Davis. MDA-MB-231 tumors bearing mice were intravenously injected through the tail vein with 4 nmol/l Cy5.5 fluorescent-labeled HEV-573C-VLPs (VLP-Cy5.5) and LXY30-conjugated HEV-573C-VLPs (LXY30-VLP-Cy5.5), respectively. At different time point (1, 6, 24 and 48 h post-injection), the mice were scanned with Kodak imaging system IS2000MM according to the procedure described previously [17]. Imaging was collected with an excitation bandpass filter at 625 nm and an emission at 700 nm at exposure time 30 s per image. After *in vivo* imaging, animals were euthanized by CO_2 overdose at 72 h after injection. Tumors, organs and muscle tissues were excised and imaged with Kodak imaging station.

Preparation of VLP–Fab complexes for cryoelectron microscopy

The VLP–Fab complexes were prepared by incubating VLPs and Fabs at a molar ratio of 1:180 at 4°C overnight. Free Fab was removed by passing VLP–Fab complex through a short Sephacryl-300 gel-filtration column. Optical density readings at a wavelength of 280 nm were used to select the fractions that contained VLP–Fab complexes.

Transmission electron microscopy

The purified VLPs were stained with 2% uranyl acetate and examined under a JOEL JEM-1230 transmission electron microscope at the magnifications of 30,000. Procedures for cryo-electron microscopy

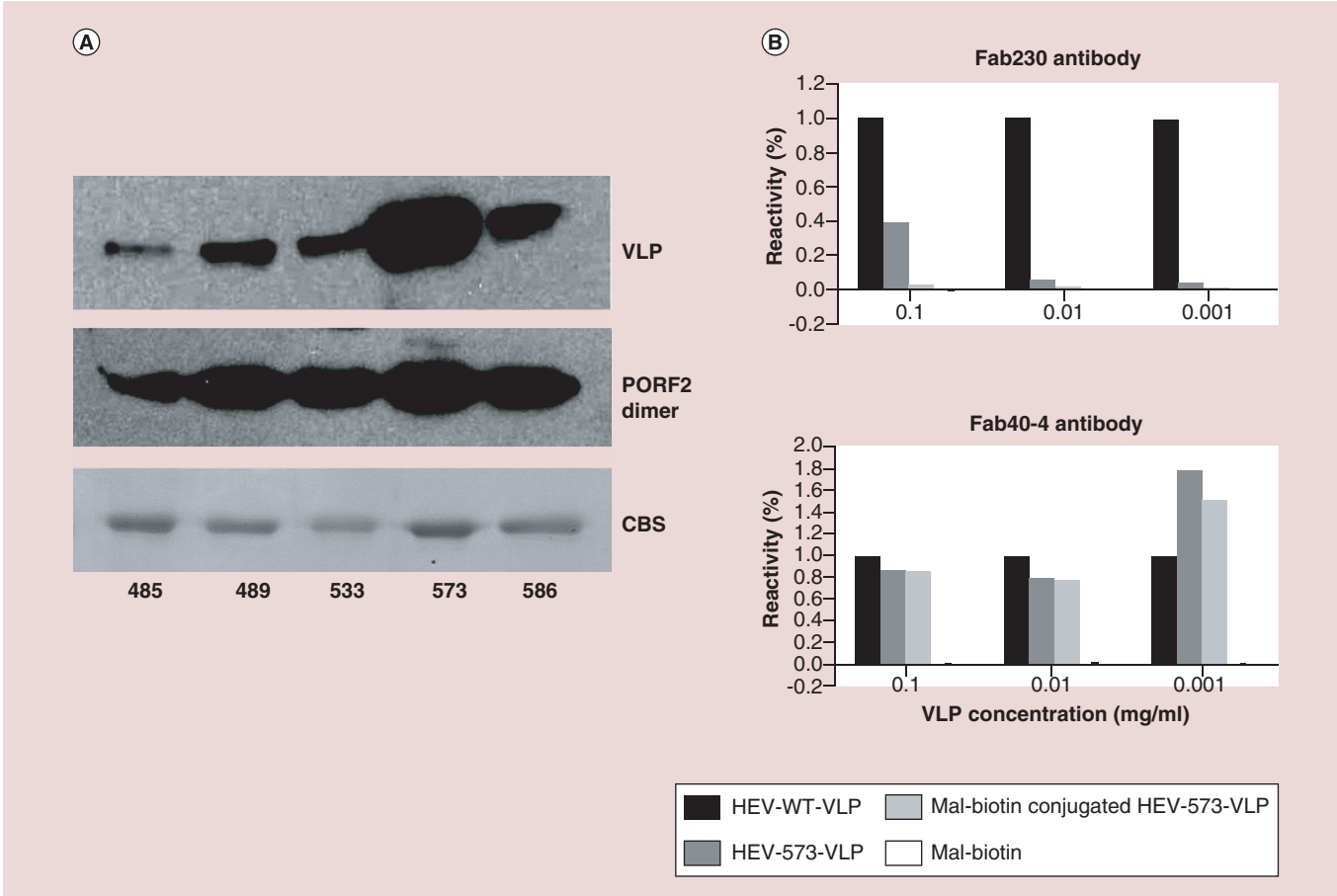

Figure 2. Characterization of chimeric virus-like particle carrying cysteine replacement. The cysteine mutation at N573 allowed efficient biotinylation to the chimeric VLP than the other mutation sites, in other words, Y485, T489, S533 and T586, although those mutations retained similar in biotinylation after VLP disassembly **(A)**. Both the wild-type VLP and the chimeric VLP were recognized by an antibody, HEP40-4B, with similar reactivity, while chimeric VLP was unreactive to antibody, HEP230 **(B)**.
CBS: Coomassie Blue staining; VLP: Virus-like particle.

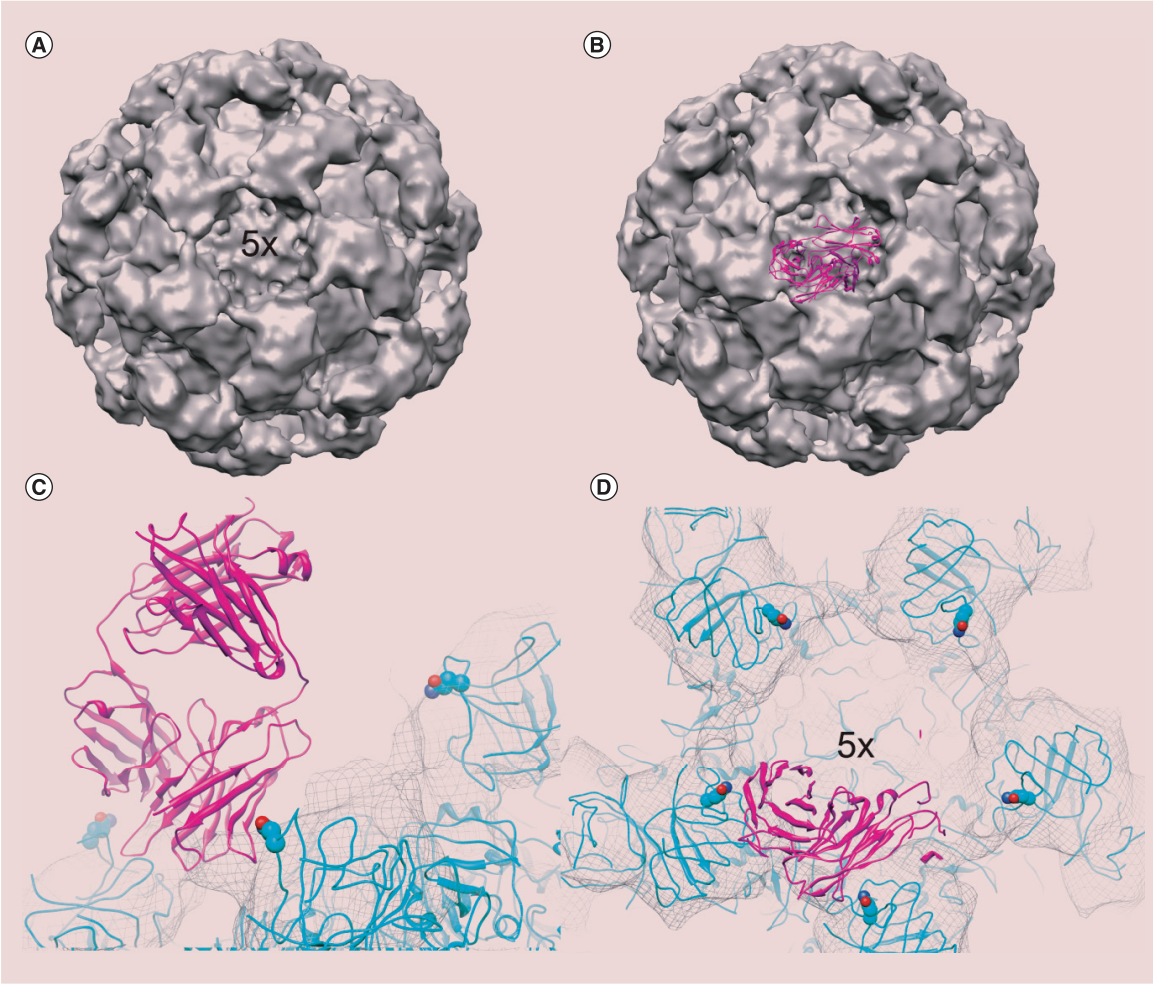

Figure 3. Residue N573 is involved in binding to HEP230. The 3D density map of HEV WT-VLP incomplexed with Fab fragments of HEP230 is displayed as isosurface along a fivefold axis, which shows extra density (red arrow) in the gap of two fivefold-related protruding dimers **(A)**. The density is in good agreement to the footprint of Fab molecule **(B)**. Residue N573 (sphere mode) is located next to the binding site of HEP230 **(C)** that allows only one Fab molecule binding per fivefold region **(D)**.

(cryo-EM) were essentially similar to that described previously [18]. Briefly, 3 µl of VLP–Fab complex was applied to a holey carbon-coated copper grid, and rapidly plunged into liquid ethane after blotting away the excess liquid. The frozen-hydrated VLP–Fab complex was then transferred into a transmission electron microscope (JEM-2100F, JEOL) equipped with a Gatan 626DH cryo holder and examined under at liquid nitrogen temperature. Micrographs were acquired under minimal dose system (<10 e/A [1]) on a TemCam-F415 CCD camera (TVIPS) at a pixel size of 2 at the specimen space.

Image processing

Particles were then manually selected and initially center and orientation was determined by reference-dependent cross-correlation by using a density of the wild-type HEV-VLP [19] as our initial model. Polar Fourier transformation algorithm [20] was used to iteratively carry out origin and orientation refinement. The contrast transfer function was determined and phase correction was applied to the data used for structural determination. 3D reconstructions were computed by combining a set of particles with orientations that spread evenly in an icosahedral asymmetric unit with superimposing the 5-3-2 icosahedral symmetry. The reliability of the reconstruction was assessed with classical Fourier Shall Correction and the final resolution was determined at 15 using 0.5 as cut-off.

Fitting of the crystal structure into cryo-electron microscopy density maps

Molecular docking was carried out with rigid body fitting the cryo-EM density map with the HEV decamer that is composed of ten of the CP (PDB 2ZZQ) using program O [21]. The fitting was evaluated based on the

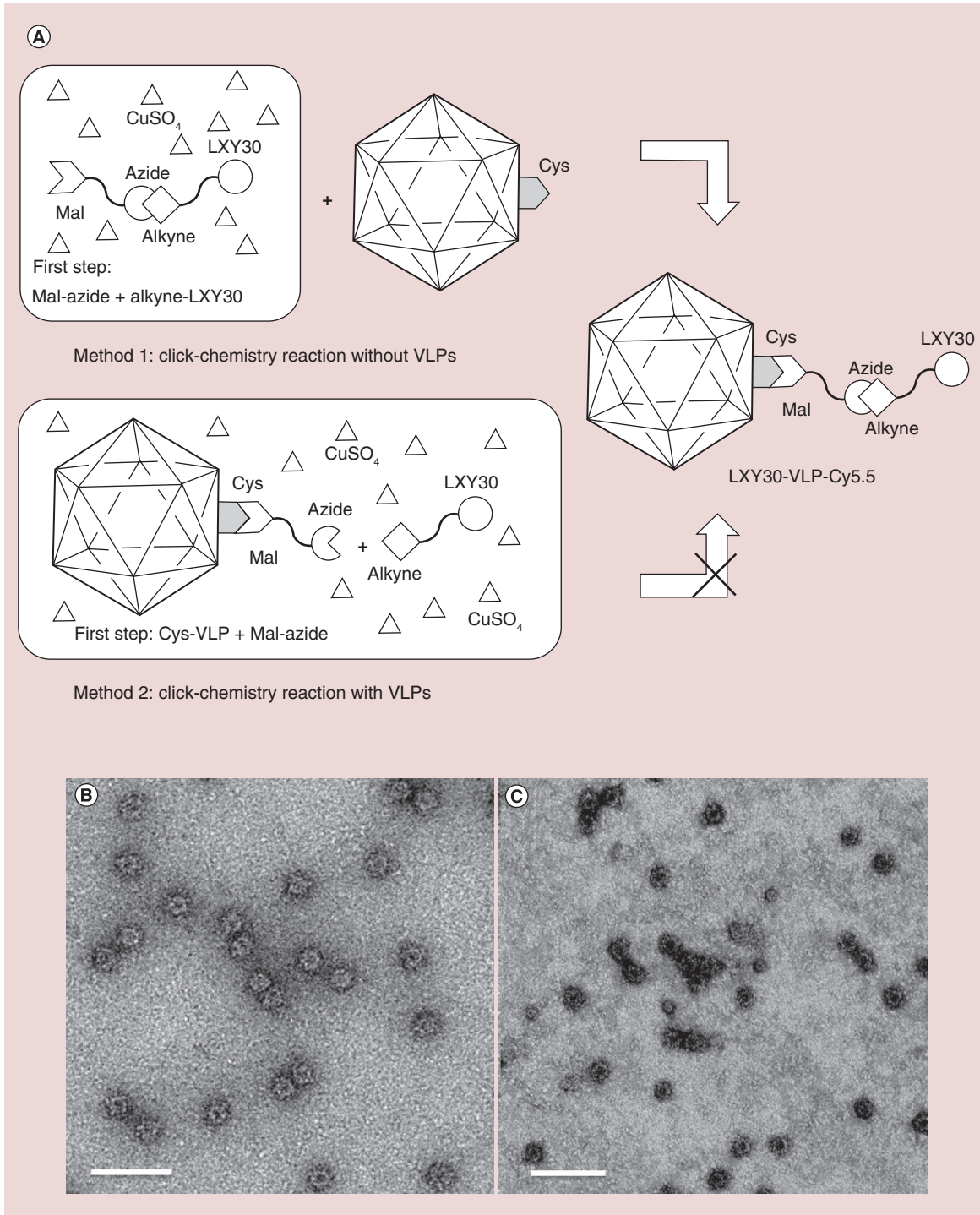

Figure 4. The schematic of the two-step chemical conjugation process including a thiol-selective reaction and a copper catalyzed azide-alkyne cycloaddition or 'click chemistry' reaction to form LXY30-virus-like particles.
Two methods have been tested in this research. Method 1: the copper catalyzed azide-alkyne cycloaddition reaction between Mal-azide and alkyne-LXY30 to form Mal-linked LXY30 (Mal-LXY30) was done first. Then the Mal-LXY30 was added to react with Cys of N573C-VLPs **(A)**. The LXY30 and Cy5.5 decorated N573C-VLP (LXY30-VLP-Cy5.5) remained intact after all these chemical conjugation processes **(B)**. Method 2: the conjugation process starting by labeling Mal-linked azide (Mal-azide) at Cys sites of N573C-VLPs through thiol-selective reaction to build azide-linked VLPs (azide-VLPs), followed by adding LXY30-alkyne, ascorbic acid and $CuSO_4$ to form LXY30-linked VLPs (LXY30-VLPs) **(A)**. However, most LXY30-VLPs were damaged or disassembled from the conjugation processes, which may be caused by the reactive reactants including azide, ascorbic acid and $CuSO_4$ **(C)**.
Mal: Maleimide; VLP: Virus-like particle.

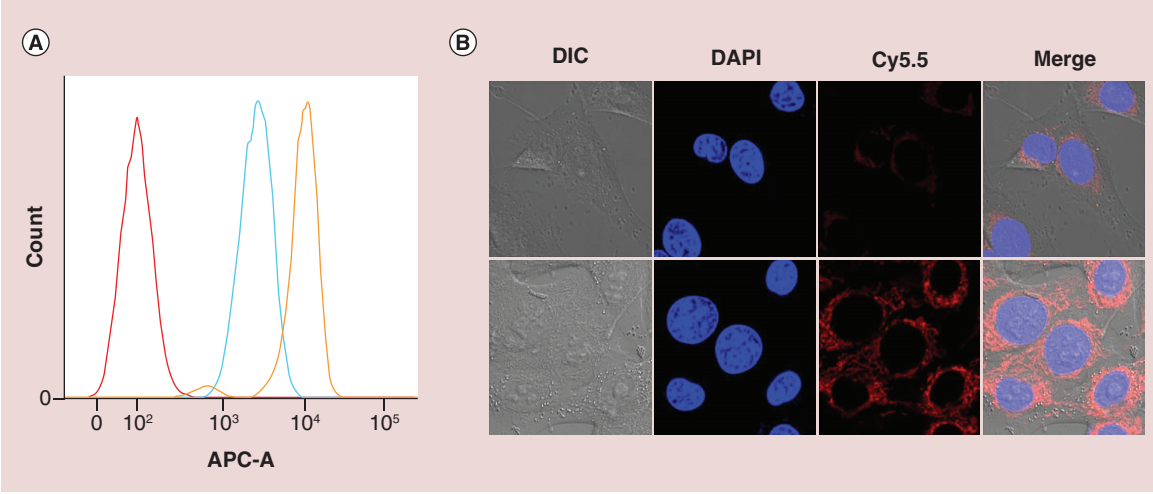

Figure 5. *In vitro* fluorescence data of virus-like particle-Cy5.5 and LXY30-virus-like particle-Cy5.5 binding to MDA-MB-231 breast cancer cells. (A) The flow cytometry data of virus-like particle-Cy5.5 or LXY3-VLP-Cy5.5 incubated with MDA-MB-231 breast cancer cells. **(B)** NIR fluorescence images of LXY30-Cy5.5-virus-like particle targeting to MDA-MB-231 cells. The signal of nuclei, which were stained by Hoechst 33342 (blue), and the signal of Cy5.5 (red) were acquired using Zeiss confocal fluorescence microscopy.

correlation coefficient between the cryo-EM map and the map computed from the fitted CP coordinates. Fitting was stopped when the correlation coefficient reached 80%. The Fab coordinates of Fab8C11 (PDB 3RKD) were used to reveal the contact footprint of Fab to HEV-VLP.

Results

Cysteine replacement at the surface loops of the P-domain

As the structure of HEV-VLP was previously established in the lab at atomic resolution [22], it was practical to select five sites for cysteine replacement from the surface variable loops of the P-domain (Figure 1). These sites were selected based on their location as well as the feasibility of sequence mutation to minimize any possible distortion of VLP assembly. As expected, individual cysteine replacement at Y485, T489, S533, N573 and T586 did not alter VLP morphology as the electron microscopy micrographs of HEV-Cys VLPs were not discernible from previously described HEV-VLP projections of 27 nm in diameter (data not shown).

To evaluate the availability for cysteine acylation, conjugation efficiency was first demonstrated between HEV-Cys VLP and maleimide-biotin, resulting in VLP biotinylation through an irreversible reaction between the maleimide and thiol group of cysteine. Among all five mutant VLPs, the VLP with a cysteine replacement at N573 (N573C-VLP) appeared to exhibit the most significant streptavidin signal following malimide–biotin conjugation (Figure 2A) Furthermore, dissembled N573C-VLP bound to malimide–biotin displayed similar streptavidin signal to the other disassembled VLP mutants (Figure 2A.) Because conjugation to N573C VLP resulted in the most exposure for secondary binding, N573C VLP was used for follow-up investigation.

The chimeric virus-like particle carrying a N573C mutation was unable to react with Hepatitis E virus antibody

Because the P-domain carries the antigenic structure of HEV, sequence mutation may alter the immunoreactivity of HEV antibodies against the obtained chimeric VLPs. To get an insight into the antigenicity of the chimeric VLPs to specific HEV antibodies, we compared the antigenicity of the chimeric N573CVLP to the wild-type HEV-VLP in the presence or absence of biotin conjugation. An ELISA plate was coated with malbiotin-conjugated and nonconjugated N573C-VLP as well as WT HEV-VLP, followed by incubation with two monoclonal antibodies, HEP230 or HEP40-4. In contrast to HEP40-4, HEP230 recognized only the wild-type HEV-VLP and failed to recognize N573C-VLP regardless of biotin conjugation (Figure 2B). The ELISA against the mixture of HEP230 and HEP40-4 showed similar trend to that previously reported for antibody HEP224 [19]. The data also suggest that residue N573 is critical to HEP230 binding.

Residue N573 is involved in antibody HEP230 binding

All of the proposed mutation residues reside in flexible loops of the P-domain, in which residues Y485, T489 and T586 are exposed on the outermost surface while residues S533 and N573 are located at the stem region of the P-domain (Figure 1B). To understand the role of residue N573 in HEP230 binding, we determined

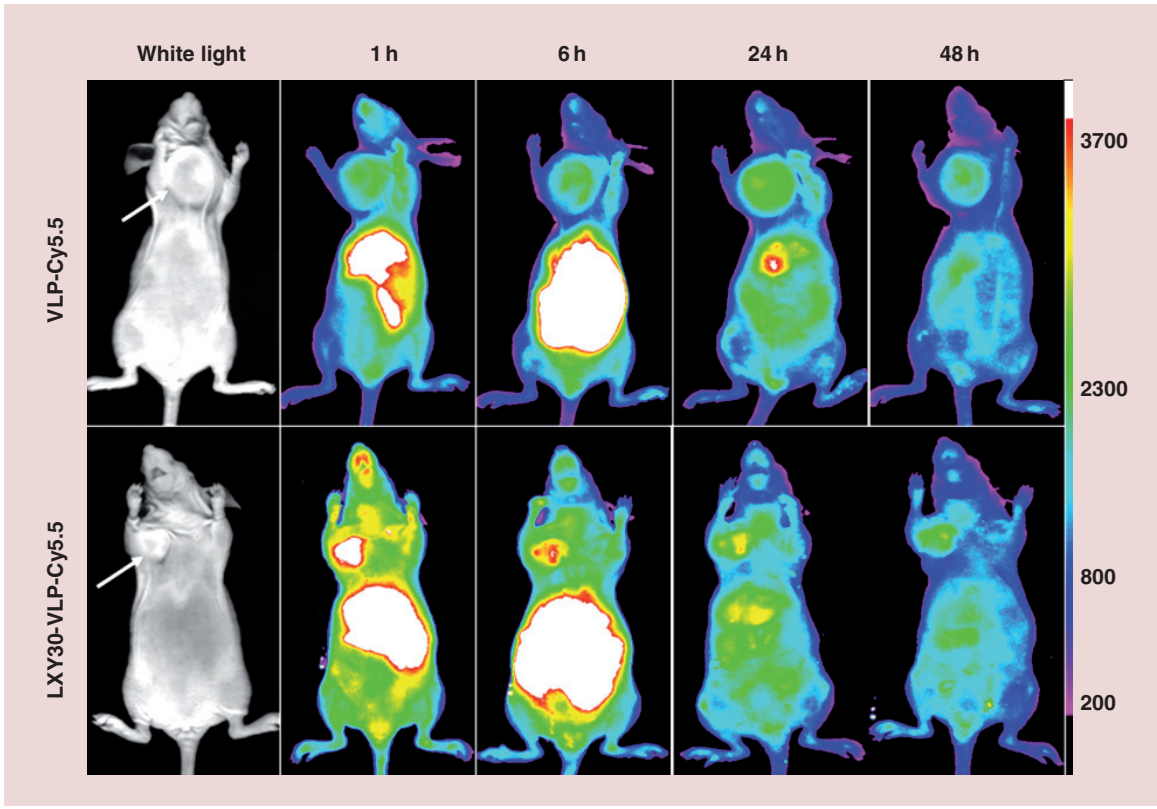

Figure 6. *In vivo* NIR fluorescence images of real-time tumor targeting characteristics of virus-like particle-Cy5.5 and LXY30-virus-like particle-Cy5.5 nanoparticles on nude mice implanted with xenografts. The MDA-MB-231 breast cancer tumor-bearing mice were injected intravenously with the equivalent amount of VLP-Cy5.5 or LXY30-VLP-Cy5.5. The tumor sites are indicated by white arrow bars. The optical imaging was obtained using Kodak multimodal imaging system IS2000MM equipped with an excitation bandpass filter at 625 nm and an emission at 700 nm.
VLP: Virus-like particle.

the complex structure of HEV-VLP with the Fab of HEP230 by cryo-EM and image processing.

N573C VLPs in complex with Fab of HEP230 (Fab230) appeared to resemble the morphology of HEV-VLP, exhibit homogeneous size distribution in cryo-electron micrographs. 3D reconstruction was calculated with superimposing icosahedral symmetry, indicating the 60 antibody-binding sites on each VLP were not fully occupied by Fab230. It revealed that HEV-VLP contained protruding spikes, each of which extend outward along icosahedral twofold axis (Figure 3A). As opposed to the native HEV-VLP, these spikes appeared to connect with each other around the icosahedral fivefold axis. The connection density between the spikes was much weaker than the capsid and was not big enough to accommodate the Fab molecule. However, the size of the connection density appeared to be in good agreement with the contacting surface of the Fab molecule (Figure 3B), indicating that the Fab230 may contact VLP at this position. This finding subsequently validated the fivefold and threefold symmetries from 3D reconstruction, in other words, using 2-2-2 symmetry instead of 5-3-2 symmetry during image processing. After five iterations of refinement, a single, slander density was observed extending from the same site of the P-domain inwardly toward the fivefold axis (data not shown). This helped to confirm that Fab230 binds to this region. Model docking with the crystal structure of a Fab fragment (PDB 3RKD) of HEV antibody 8C11 revealed that the extra density did cover the three contact loops in the Fab (Figure 3C). Docking the crystal structure of HEV CP (PDB 1ZZQ) into the density map revealed that residue N573 is in the binding footprint of Fab230 (Figure 3C & D), and could be in direct contact with the residues from Fab230.

LXY30-conjugated N573C virus-like particles showed cancer cell targeting

To assess the targeting and diagnostic capability of N573-VLP, a breast cancer cell targeting ligand, LXY30, was chemically added to the surface N573C-VLPs through a cysteine-anchored melamine-alkyne. LXY30 is a cyclic peptide, derived from LXY3, with enhanced affinity to α-3 integrin on MDA-MV-231

breast cancer cells [11]. Although LXY30-maleimide coupling provides one-step conjugation to N573-VLP, click chemistry was introduced to conjugate ligand to VLP, as an attempt of ligation to a variety of molecules, especially the synthetic peptides or oligosaccharides. As the anchor, maleimide-azide coupling with VLP can be performed prior to cycloaddition with alkyne-linked ligand (method 2), or after cycloaddition (method 1) (Figure 4A). Our results showed that the method 1 did not cause VLP deformation (Figure 4B), while the method 2 disrupted VLP (Figure 4C). Flow cytometry revealed a significantly higher attachment (more than fivefolds) for LXY30-VLPs to MDA-MB-231 breast cancer cells, as compared with that for the wild-type VLPs (Figure 5A), indicating that LXY30-VLP specifically targets breast cancer cells.

To determine if LXY30-VLPs enters the MDA-MB-231 cells, the distribution of CP was observed after incubation of LXY30-VLPs and MDA-MB-231 cells by the confocal microscopy. For this imaging, the LXY30-VLPs were labeled with the near infrared dye, Cy5.5, and incubated with MDA-MB-231 cells at 37°C for 1 h. As shown in Figure 5B, most Cy5.5-labeled VLPs distributed around the perinuclear region of MDA-MB-231 cells, which meant the VLP was internalized into the cytoplasm. Wild-type VLPs had minimal cellular uptake, whereas LXY30-VLPs exhibited significantly higher uptake in MDA-MB-231 cells (Figure 5B). These results demonstrated that the chemical conjugation with target ligand is capable of eliciting the specific uptake of HEV-VLP into breast cancer cells.

Targeting of LXY30-conjugated N573C virus-like particles in breast tumor *in vivo*

Noninvasive *in vivo* imaging has been shown to be a powerful tool to visually monitor the delivery of therapeutic reagents. *In vivo* near infrared (NIR) optical imaging was used to investigate the distribution of the VLPs in nude mice bearing MDA-MB-231 breast cancer xenografts, as a criterion to evaluate the specificity of tumor targeting. Both Cy5.5-labeled LXY30-VLPs and the Cy5.5-labeled wild-type VLPs were intravenously injected via tail vein in nude mice bearing MDA-MB-231 xenografts, respectively. The mice were scanned with the fluorescence imager at various intervals for up to 72 h. Both Cy5.5-labeled wild-type VLPs and LXY30-VLPs distributed throughout the body of the mice immediately after

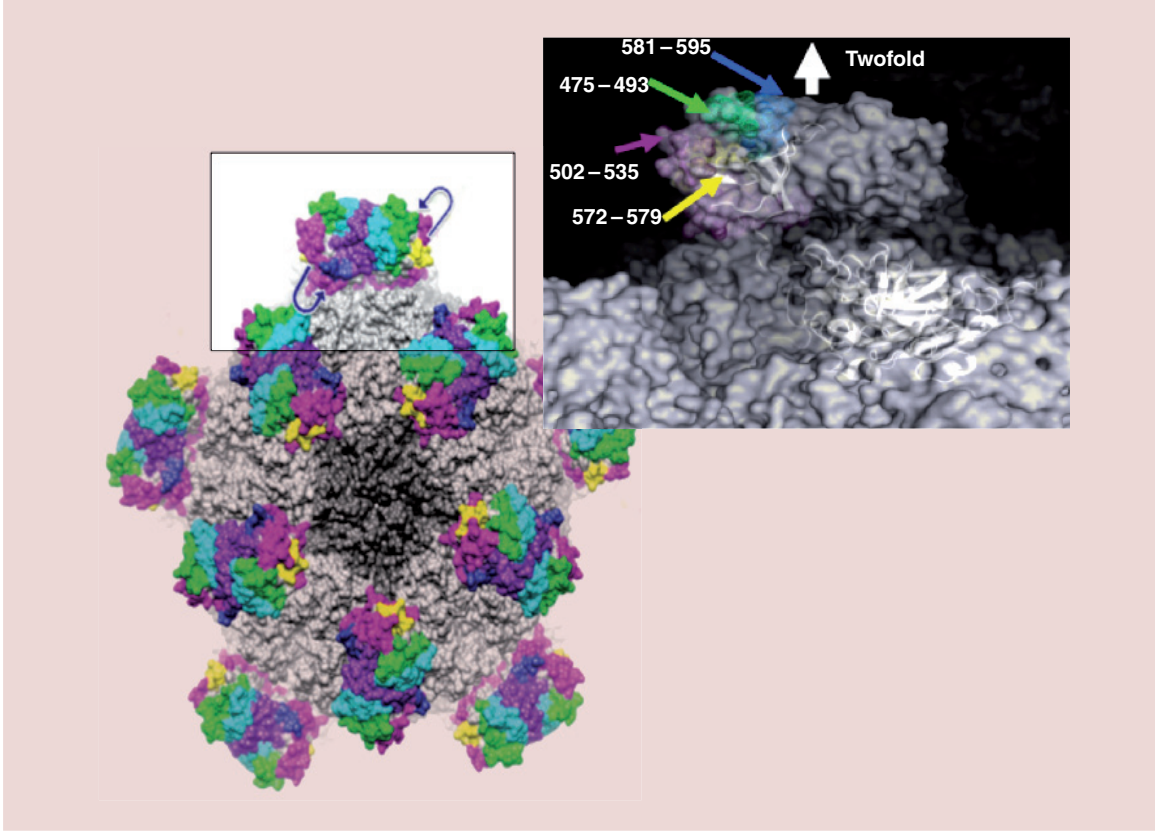

Figure 7. The surface representation of hepatitis E virus-virus-like particle. The P-domain (boxed region) is expanded on the right to depict surface variable loop residues and C-terminal residue. One or more cysteines can be positioned within the indicated loop or C-terminal residues for conjugation to a molecular payload.

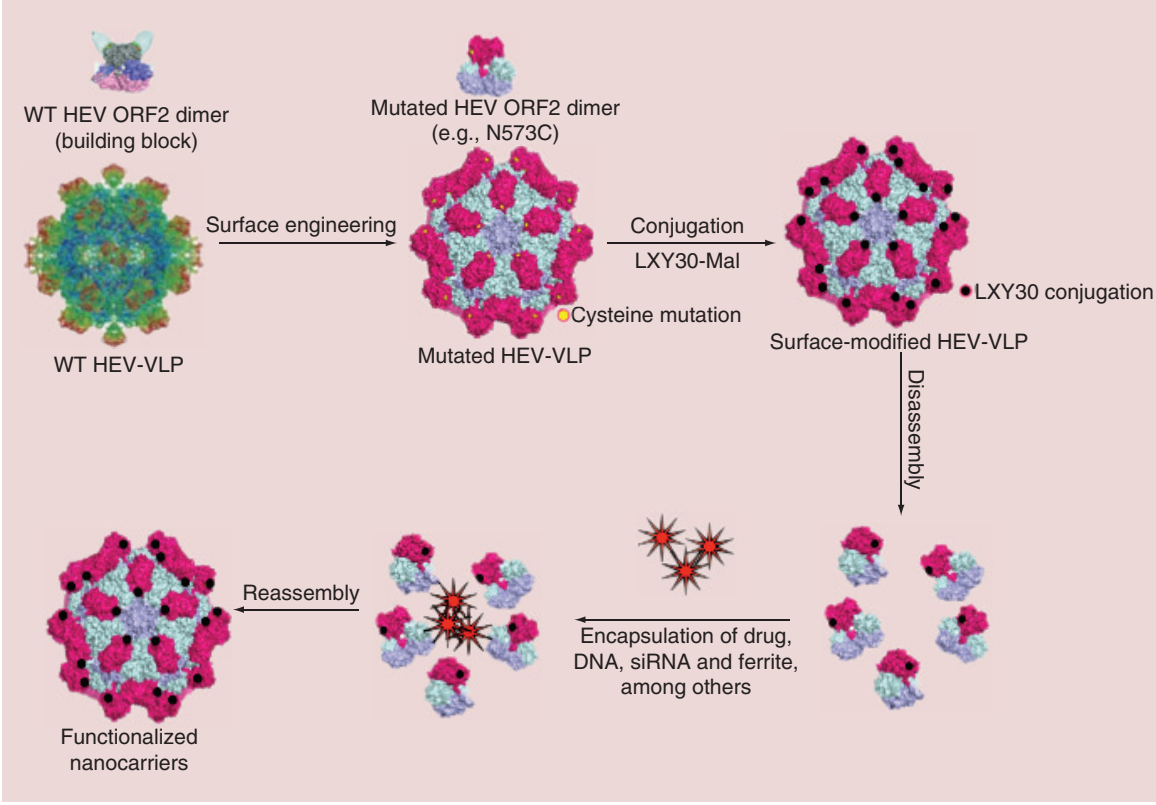

Figure 8. Schematic depicting the application of chimeric hepatitis E virus-virus-like particles as nanocarriers for drug delivery. The periodicity of the capsid, the presence of surface-accessible amino acids with reactive moieties, and the tolerance of a single-chain version of the capsid protein dimer to diverse peptide insertions enable dense, repetitive display of targeting ligands either by chemical conjugation or genetic insertion, and display of aptamers or glycoproteins by chemical conjugation. HEV VLPs also possess relatively large interior volumes that can be loaded with a variety of materials, including DNA plasmids. In comparison with other VLPs, HEV VLPs possess strong structural plasticity, with a stability switch sensitive to calcium concentration.
HEV: Hepatitis E virus; Mal: Maleimide; VLP: Virus-like particle; WT: Wild-type.

the intravenous injection, and gradually accumulated into the MDA-MB-231 tumor via the enhanced permeability and retention effect. However, the uptake rate of LXY30-VLPs in the tumor site was faster than that of wild-type VLPs. The fluorescence intensity of Cy5.5-labeled LXY30-VLPs in MDA-MB-231 tumor was significantly higher than that of Cy5.5-labeled wild-type VLPs at 1 and 6 h post-injection (Figure 6). HEV, as an enteric transmitted virus, preferentially enters hepatocytes in liver. It is not surprising that Cy5.5-labeled VLPs accumulated within 1 h at the abdominal organs including liver. *Ex vivo* imaging of excised organs was performed at 72 h post-injection. The remaining signal of Cy5.5 was found dominantly at liver and kidney, however, appeared weak in excised tumor (data not shown). The high uptake in liver and kidney could be explained in part as leaking of the breakdown VLPs from circulating vessels. Overall, these results indicate that Cy5.5/LXY30-linked HEV-VLPs are able to relatively target MDA-MB-231 xenografts *in vivo*.

Discussion

For diseases such as cancer, the need of the hour is to formulate drug delivery modalities that have the ability of tumor-specific targeting. The VLP is a platform that provides not only the solution of cargo encapsulation, but also an opportunity for tissue/cell-specific approaches while minimizing the overall damage to healthy cells [23,24]. Compared with other nano-delivery systems that have a limited half-life due to early degradation, HEV is a feco-orally transmitted virus, and HEV-VLPs, which resemble the virus, can maintain their structure through a variety of harsh environmental conditions. The stable nature of the capsid implies that the VLP does not require refrigeration for storage. Previous studies from our lab have also demonstrated that chimeric HEV-VLPs retain their state of assembly even on exposure to intestinal proteases like trypsin [10]. This implies that the theranostic capsule can be delivered orally. There is an immense ease in oral administration of cancer therapy, particularly for patients who are unfit for clinic visits and repeated

vein punctures. This stability is particularly advantageous in the context of increased bioavailability when used as an oral chemotherapeutic agent. HEV-VLPs could thus have a higher propensity for efficient delivery and reduced accumulation due to particle degradation [14], both properties being critical factors for therapeutic nanocarriers.

The baculovirus expression vector-based production of CP in commercially available insect High Five cells generates HEV-Cys-VLP capsid protein that is easily purified at high yield and low cost [25]. In contrast, many other nanodelivery systems are compromised due to variable expression levels and inefficiency in production.

Common bioconjugation reactions involve ligation to lysine residues with NHS or to cysteine residues with maleimide. The former approach is nonspecific because there are many lysine residues on proteins. Here a cysteine residue was genetically engineered to be exposed on the surface of the HEV-VLP P-domain, allowing acylation to anchor an external ligand to a single, most exterior site. To avoid the competition, the conjugation of a near-infrared dye, Cy 5.5 was performed by amine-coupling, with the purpose to detect VLP distribution in cells and *in vivo*.

Five sites were chosen for replacement with cysteine – these were Y485C, T489C, S533C, N573C and T586C (Figure 7). The mutant constructs were seen to retain their ability to form VLPs, as observed by transmission electron microscopy. The mutants were conjugated to biotin-maleimide, their usability as theranostic capsules was assessed based on accessibility of the conjugated biotin to its ligand, streptavidin. Among all of the chimeric VLPs that we generated, N573C-VLP construct appeared to show the strongest streptavidin binding, despite the fact that the cysteine thiol group is embedded within the surface depression at icosahedral fivefold axis. Structural analysis revealed that the distance between N573C and its fivefold related neighboring N573C is 45A, a distance that is in a good agreement with the length of a streptavidin monomer. In fact, the streptavidin is a homotetramer in solution. The streptavidin homotetramer can intercalate into the surface depression and form multivalent interaction with N573C-anchored biotin molecules, which largely reduces the rate of dissociation. As a result, the avidity of streptavidin to N573C-VLP is the highest although the affinity of streptavidin to a single biotin appeared to be the same as it showed by its binding to the disassembled VLPs. By contrast, the quaternary arrangement of cysteine residues in the other chimeric VLPs does not support multivalent binding of streptavidin.

HEV-N573C-VLP was subsequently found effective in avoiding nonspecific ligand bindings to the HEV P-domain, although the four endogenous lysine residues were potentially accessible from the capsid surface. In conjunction with cysteine conjugation, alkylation was used to simultaneously bind fluorescent molecules to exposed lysine residues for VLP tracking.

The N573 residue is located within the binding footprint of the Fab230, so that mutation of N573 blocks the interaction of CP and HEP230. However, the volume of a fivefold depression is not sufficient so as to simultaneously accommodate five Fab molecules. Thus, the structure of Fab-bound VLP can only capture the contacting region of the Fab molecule after icosahedral average. The density is about 20% occupancy to that of the capsid, suggesting that only one Fab molecule resided at each fivefold axis. This is consistent with the nonicosahedral symmetry averaged density map. This binding site is different to our previously reported binding site for antibody HEP224, whose binding depends critically on residue Y485 of CP [26]. The reconstruction of HEP224-bound VLP revealed density of 60 Fabs at the shoulder of the P-domain with Fab extending away from VLP center [26]. This suggests of two distinctive antigenic domains on the surface of HEV-VLP that do not overlap with each other; in agreement with the results of ELISA [19]and mutagenesis result [13] that were previously reported for HEV.

After extensive characterization of the HEV-N573C-VLP, we conjugated it to a breast cancer targeting ligand, LXY30, by thiol-selective coupling. LXY30 is a ligand for binding to integrin α-3 (ITGA3 or CD49C), and is highly overexpressed on the surface of breast carcinoma tissues [11]. The LXY30 HEV-VLP was subsequently labeled to fluorophore Cy5.5 to trace its trafficking in cells and *in vivo*. To this end, we found the binding of the LXY30-conjugated HEV-VLPs to be significantly higher on the surface of breast cancer cell line MDA-MB-231, as compared with unconjugated, Cy5.5-labeled VLP. Further, internalized VLP was largely perinuclear, and internalization of LXY30-conjugated VLPs was significantly more as compared with the unconjugated VLP.

Last, we administered the conjugated or unconjugated VLP in mice that had previously received a xenograft of breast cancer cells. The LXY30-conjugated VLP accumulated in the tumor tissue at a higher level as compared with unconjugated VLP. However, there was significant nonspecific uptake of the capsule in liver and kidney, and this would pose as a serious side effect for medical applications. This problem could be solved by a variety of approaches [27,28], including fur-

ther engineering of the VLP surface. We are currently in the process of evaluating one such modification, for better targeting to cancer cells with nonspecific tissue accumulation *in vivo*.

Conclusion

We developed an orally deliverable, protein-based nanoparticle based on the structure of hepatitis E virus. The capsid protein was expressed in insect cells to produce the VLP carrying the site-directed cysteine mutation in one of the five designated loops on the protrusion domain. This allowed surface modification through thiol-based coupling to the mutated and surface-exposed cysteine residue. Of the five mutants, we found that N573C showed the maximum degree of surface conjugation, although all the mutants formed VLPs. We conjugated the breast cancer-targeting ligand LXY30 to the N573C VLP, and amine coupled a NIR dye to track the VLP movement. The LXY30 VLP bound to breast cancer cells in culture to a much higher extent as compared to unconjugated VLP. Furthermore, it targeted the breast cancer tissue *in vivo* more efficiently than the unconjugated VLP. This platform will enable oral administration of a cheap cancer-targeting nanoparticle that can carry therapeutic or diagnostic agents

Future perspective

A modularized theranostic capsule, targeting breast tumor, was constructed to demonstrate the potential cancer diagnostic and potential therapeutic application utilizing an HEV-VLP platform. Besides conjugating the cancer cell targeting ligand on the surface, the utilization of modularized theranostic capsule can be expanded by using the interior space of Cys-VLPs as well. Citric acid coated ferrite particles had been successfully encapsulated into HEV-VLPs using *in vitro* capsid reassembly, which can be detected in mice by MRI. It could also be applied to tumor-targeted hyperthermia induced by ultrasound or radio frequency electromagnetic radiation using heat-activated ferrite particles encapsulated in the tumor-targeted theroanostic capsule [29]. Another exciting application to be explored is based on the prior finding that negatively charged micro-RNA/siRNA could be also encapsulated into the interior of HEV-Cys-VLPs [30]. Packaging the micro-RNA/siRNA targeting genes to be silenced interiorly, the proposed therapeutic capsule can be an effective carrier for cancer-targeted gene therapy (Figure 8). By binding the cancer cell targeting ligand on its surface, HEV-Cys-VLP could have potential applications in cancer cell targeting gene therapy; consequently, this would improve current treatments used in cancer patients.

Acknowledgements

The authors thank Y Izumiya for sharing Sf9 insect cells and advices in insect cell culture, as well as T Li for the sharing of an antibody reagent.

Financial & competing interests disclosure

This work is supported in part by the NIH Research Grant (AI095382, EB021230, CA198880), National Institute of Food and Agriculture, Neobio Immune Fund and Discovery Grant

Executive summary

Background

- Genetically engineered hepatitis E virus (HEV) virus-like particles (VLPs) can be surface modified without compromising their stability.
- Either of five key residues of the surface variable loops of the HEV capsid protein was replaced with cysteine to allow thiol-selective conjugation between maleimide and cysteine.

Methods

- Either of five sites on the protrusion domain of the HEV VLP were mutated, and expressed in insect cells to produce VLPs in the supernatatnt.
- Of the five engineered VLPs, N573C VLP was best suited for further modification, and it was conjugated to the breast cancer targeting ligand, LXY30.

Results

- The N573C VLP conjugated to LXY30 breast cancer targeting ligand and allowed to bind to breast cancer cell line MDA-MB-231, as well as cell-line-derived xenografts in mice. LXY30 VLP bound to a higher extent in cell line as well as in tumor tissue as compared with wild-type VLP.

Conclusion

- The HEV VLP can be engineered to be surface-modified without compromising the integrity of the particle.
- Further, engineering allows diverse functional groups to be displayed on the surface of the VLPs, which can then be used to target to various specialized cells and tissues, such as cancer cells.
- LXY30, a breast cancer targeting ligand, can be conjugated to the N573C HEV VLP to specifically target to breast cancer cells and *in vivo* in mice. This can be a powerful platform to develop theranostic nanoparticles for oral delivery and targeting to tumor tissues.

(Bio 05-10505) to RH Cheng. This study is in part the fulfillment of C-C Chen's PhD degree (under the supervision of Y-H Hsu and N-S Lin) sponsored by Molecular and Biological Agricultural Sciences Program, Taiwan International Graduate Program, Academia Sinica and the Graduate Institute of Biotechnology, National Chung-Hsing University. The authors have no other relevant affiliations or financial involvement with any organization or entity with a financial interest in or financial conflict with the subject matter or materials discussed in the manuscript apart from those disclosed.

No writing assistance was utilized in the production of this manuscript.

Ethical conduct of research

The authors state that they have obtained appropriate institutional review board approval or have followed the principles outlined in the Declaration of Helsinki for all human or animal experimental investigations. In addition, for investigations involving human subjects, informed consent has been obtained from the participants involved.

References

1 Ludwig C, Wagner R. Virus-like particles-universal molecular toolboxes. *Curr. Opin. Biotechnol.* 18, 537–545 (2007).

2 Ahmad I, Holla RP, Jameel S. Molecular virology of hepatitis E virus. *Virus Res.* 161(1), 47–58 (2011).

3 Yu H, Li S, Yang CY *et al.* Homology model and potential virus-capsid binding site of a putative HEV receptor Grp78. *J. Mol. Model.* 17(5), 987–995 (2011).

4 Gu T, Liu Z, Ye Q *et al.* Structure of the hepatitis E virus-like particle suggests mechanisms for virus assembly and receptor binding. *Proc. Natl Acad. Sci. USA* 106, 12992–12997 (2009).

5 Xing L, Li TC, Miyazaki N *et al.* Structure of hepatitis E virion-sized particle reveals an RNA-dependent viral assembly pathway. *J. Biol. Chem.* 285, 33175–33183 (2010).

6 Yamashita T, Mori Y, Miyazaki N. Biological and immunological characterics of hepatitis E virus-like particles based on the crystal structure. *Proc. Natl Acad. Sci. USA* 106, 12986–12991 (2009).

7 Xing L, Kato K, Li T *et al.* Recombinant hepatitis E capsid protein self-assembles into a dual-domain T = 1 particle presenting native virus epitopes. *Virology* 265(1), 35–45 (1999).

8 Li S.W, Zhang J, Li Y *et al.* A bacterially expressed particulate hepatitis E vaccine: antigenicity, immunogenicity and protectivity on primates. *Vaccine* (22), 2893–901 (2005).

9 Niikura M, Takamura S, Kim G *et al.* Chimeric recombinant hepatitis E virus-like particles as an oral vaccine vehicle presenting foreign epitopes. *Virology* 293(2), 273–280 (2002).

10 Jariyapong P, Xing L, van Houten NE *et al.* Chimeric hepatitis E virus-like particle as a carrier for oral-delivery. *Vaccine* 31(2), 417–424 (2013).

11 Yao N, Xiao W, Wang X. Discovery of targeting ligands for breast cancer cells using the one-bead one-compound combinatorial method. *J. Med. Chem.* 52(1), 126–133 (2009).

12 Li TC, Yamakawa Y, Suzuki K *et al.* Expression and self-assembly of empty virus-like particles of hepatitis E virus. *J. Virol.* 71(10), 7207–7213 (1997).

13 Nilsson J, Miyazaki N, Xing L *et al.* Structure and assembly of a T=1 virus-like particle in BK polyomavirus. *J. Virol.* 79(9), 5337–5345 (2005).

14 Merrington CL, King LA, Possee R.D. Baculovirus expression systems. In: *Protein Expression: A Practical Approach.* Higgins SJ, Hames BD (Eds). Oxford University Press, USA, 101–127 (1999).

15 Li TC, Takeda N, Miyamura T *et al.* Essential elements of the capsid protein for self-assembly into empty virus-like particles of hepatitis E virus. *J. Virol.* 79(20), 12999–13006 (2005).

16 Xiao K, Li Y, Lee JS *et al.* "OA02" peptide facilitates the precise targeting of paclitaxel-loaded micellar nanoparticles to ovarian cancer in vivo. *Cancer Res.* 72(8), 2100–2110 (2012).

17 Luo J, Xiao K, Li Y *et al.* Well-defined, size-tunable, multifunctional micells for efficient paclitaxel delivery for cancer treatment. *Bioconjug. Chem.* 21, 1216–1224 (2010).

18 Kawano MA, Xing L, Tsukamoto H *et al.* Calcium bridge triggers capsid disassembly in the cell entry process of simian virus 40. *J. Biol. Chem.* 284(50), 34703–34712 (2009).

19 Jariyapong P, Xing L, van Houten NE. Chimeric hepatitis E virus-like particle as a carrier for oral-delivery. *Vaccine* 31(2), 417–24 (2013).

20 Baker T, Cheng H. A model based approach for determining orientations of biological macromolecules imaged by cryo-electron microscopy. *J. Struct. Biol.* 116, 120–130 (1996).

21 Jones TA, Zou JY, Cowan SW, Kjeldgaard M. Improved method for building protein model in electron density maps and the location of errors in these models. *Acta Crystallogr. A* 47, 110–119 (1991).

22 Xing L, Li TC, Miyazaki N. Structure of hepatitis E virion-sized particle reveals an RNA-dependent viral assembly pathway. *J. Biol. Chem.* 285, 33175–33183 (2010).

23 Galaway FA, Stockley PG. MS2 viruslike particles: a robust, semisynthetic targeted drug delivery platform. *Mol. Pharm.* 10(1), 59–68 (2013).

24 Ma Y, Nolte RJ, Cornelissen JJ. Virus-based nanocarriers for drug delivery. *Adv. Drug Deliv. Rev.* 64(9), 811–25 (2012).

25 Kawano M, Xing L, Lam KS *et al.* Design platforms of nanocapsules for human therapeutics or vaccine In: *Development of Vaccines.* Singh M, Srivastava IK, (Eds). Wiley Publishing, NJ, USA, 125–140 (2011).

26 Xing L, Wang JC, Li TC *et al.* Spatial configuration of hepatitis E virus antigenic domain. *J. Virol.* 85(2), 1117–24 (2011).

27 Chen S, Cao Z, Jiang S. Ultra-low fouling peptide surfaces derived from naturalamino acids. *Biomaterials* 30(29), 5892–5896 (2009).

28 Jiang S, Cao Z. Ultralow-fouling, functionalizable, and hydrolyzable zwitterionic materials and their derivatives

for biological applications. *Adv. Mater.* 22(9), 920–932 (2010).

29 Roemer RB. Engineering aspects of hyperthermia therapy. *Annu. Rev. Biomed. Eng.* 1, 347–76 (1999).

30 Takamura S, Niikura M, Li TC *et al.* DNA vaccine-encapsulated virus-like particles derived from an orally transmissible virus stimulate mucosal and systemic immune responses by oral administration. *Gene Ther.* 11(7), 628–635 (2004).